IOP Publishing Physica Scripta
Phys. Scr. **81** (2010) 025502 (6pp) doi:10.1088/0031-8949/81/02/025502

Plasma effects in a travelling wave tube

Manish Kumar, Lalita Bhasin and V K Tripathi

Physics Department, Indian Institute of Technology, Delhi 110016, India

E-mail: kumarmanish21@hotmail.com

Received 1 October 2009
Accepted for publication 14 December 2009
Published 13 January 2010
Online at stacks.iop.org/PhysScr/81/025502

Abstract
The effect of a plasma on a travelling wave tube comprising a sheath helix is studied. The plasma, taken to be (i) strongly magnetized or (ii) unmagnetized, allows a larger beam current to pass owing to charge and current neutralization. The beam excites an azimuthally symmetric slow wave via Cerenkov resonance. In the case of a strongly magnetized plasma when $\omega_p > \omega$ (where ω_p is the plasma frequency), the amplitude of the axial electric field peaks on the axis and the phase velocity is suppressed, whereas for $\omega_p < \omega$ the field amplitude peaks at the helix surface and the phase velocity is enhanced. As a consequence, when a beam is placed close to the helix, the growth rate increases with ω_p as long as $\omega_p < \omega$ and decreases with ω_p when $\omega_p > \omega$. In the case of an unmagnetized plasma, the mode is more strongly localized near the helix and the growth rate increases with ω_p.

PACS numbers: 52.25.Xz, 52.40.Fd, 52.59.Ye

(Some figures in this article are in colour only in the electronic version.)

1. Introduction

The travelling wave tube (TWT) [1] continues to be the most widely used source of broad-band high-power microwave generation at centimetre wavelengths. An electron beam passing through a slow wave structure excites a slow electromagnetic wave whose phase velocity closely equals the velocity of the beam. This phenomenon of Cerenkov emission is the basis for all TWTs. In order to have broad bandwidth microwave amplification, one frequently uses slow wave structures, such as a partially dielectric-loaded waveguide [2], a disc-loaded waveguide or a helix [3], which slow down the phase velocity of the electromagnetic wave. In this regard, Chu and Jackson [4] have given a very elegant linear theory of TWTs treating the helix as an anisotropic conducting surface. Uhm and Choe [3] examined the properties of the electromagnetic wave propagation through a helix-loaded waveguide. Several authors later considered different aspects of TWT devices. However, a common feature of all these theories is that they consider only one-dimensional motion of electrons and ignore the effects of any background plasma.

As a matter of fact, the residual gases in the guiding system get ionized by the beam and a plasma of appreciable density is formed. Unless the vacuum is kept very high, the plasma density may be comparable to or even larger than the density of the beam. This should provide some degree of charge neutralization and thus an e-beam with higher current can propagate and also guide the beam without requiring a very strong guide field. Tripathi [5] has considered the effect of plasma in a partially dielectric-loaded parallel plane guiding system. The plasma modifies the mode structure considerably, leading to a reduction in the growth rate and hence in the efficiency of the device. Talukdar and Tripathi [6] have studied the excitation of whistler modes in a cylindrical plasma column by a solid electron beam. The helix slows down the whistler mode and relaxes the requirements on the beam energy for the generation of a given frequency. Pant and Tripathi [7] have reported that a plasma-loaded sheath helix supports lower hybrid modes that extend outside of the vacuum region. An analysis of lower hybrid mode excitation by a beam propagating in the vacuum region reveals that nonlocal effects significantly reduce the growth rate.

In this paper, we study the excitation of slow electromagnetic waves in a plasma-loaded sheath helix. We consider a sheath helix filled with (i) a strongly magnetized plasma and (ii) an unmagnetized plasma. In the first situation, the plasma is strongly anisotropic, whereas in the second it is isotropic. In section 2, we obtain the beam and plasma response to electromagnetic fields of a mode. In section 3, we study the mode structure. In section 4, we introduce the beam term into the wave equation and evaluate the growth rate of the slow wave mode. The results are briefly discussed in section 5.

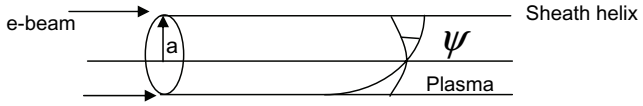

Figure 1. System configuration.

2. Beam and plasma response

Consider a sheath helix of radius a_1 and pitch angle ψ filled with plasma of density n_p^o (see figure 1). The helix is considered as an anisotropically conducting cylinder with infinite conductivity along the wire of the helix and zero conductivity across it. This is reasonable as long as the phase change over each element of length L of the periodic structure is considerably less than π. The plasma is cold and uniform and is subjected to an axial magnetic field $B_s\hat{z}$. We consider two cases: (i) B_s is very strong so that the plasma dynamics are one dimensional and (ii) when B_s is very weak so that the plasma is isotropic. A thin hollow cylindrical electron beam of radius a and density $n_b^o = N_b\delta(r-a)$ passes through the plasma with velocity $v_{ob}\hat{z}$. An azimuthally symmetric microwave eigenmode of the system has electric and magnetic fields

$$\vec{E} = \vec{A}(r)e^{-i(\omega t-kz)},$$
$$\vec{B} = \vec{A}'(r)e^{-i(\omega t-kz)}.$$

The beam and plasma responses to these fields are governed by the equation of motion

$$m\left[\frac{\partial\vec{v}}{\partial t}+(\vec{v}\cdot\nabla)\vec{v}\right] = -e\vec{E}-\frac{e}{c}\vec{v}\times\vec{B}, \tag{1}$$

where $-e$ and m are the electronic charge and mass. For beam electrons when $\omega - kv_{ob} \ll \omega_c$, where ω_c is the electron cyclotron frequency, only the $\hat{z}$-component of velocity is important and it turns out to be

$$v_{1bz} = \frac{eE_z}{mi(\omega-kv_{ob})}. \tag{2}$$

Linearizing the equation of continuity

$$\frac{\partial n_b}{\partial t}+\nabla\cdot(n_b\vec{v}_b) = 0, \tag{3}$$

one obtains the density perturbation

$$n_{1b} = \frac{n_b^o ekE_z}{mi(\omega-kv_{ob})^2}. \tag{4}$$

The perturbed beam current density can be written as

$$\vec{J}_b = -n_b^o e\vec{v}_b - n_b e\vec{v}_{ob}, \tag{5}$$

$$= -\frac{n_b^o e^2\omega E_z}{mi(\omega-kv_{ob})^2}\hat{z}. \tag{6}$$

The response of plasma electrons in the limit $\omega \ll \omega_c$ can also be taken to be one-dimensional and can be recovered from the beam response by taking $v_{ob} = 0$ and replacing beam parameters by plasma parameters

$$\vec{J}_p = -\frac{n_p^o e^2}{mi\omega}E_z\hat{z}. \tag{7}$$

In the opposite limit $\omega \gg \omega_c$, the plasma is unmagnetized, and one can write

$$\vec{J}_p = -\frac{n_p^o e^2}{mi\omega}\vec{E}. \tag{8}$$

3. Mode structure

The wave equation for the mode is

$$\nabla^2\vec{E}-\nabla(\nabla\cdot\vec{E})+\frac{\omega^2}{c^2}\underline{\underline{\varepsilon}}\cdot\vec{E} = -\frac{4\pi i\omega}{c^2}\vec{J}_b, \tag{9}$$

where $\underline{\underline{\varepsilon}}$ is the dielectric tensor. For the strongly magnetized case $(\omega, \omega_p \ll \omega_c)$, $\varepsilon_{xx} = \varepsilon_{yy} = 1$, $\varepsilon_{zz} = 1-\omega_p^2/\omega^2$ and $\varepsilon_{xy} = \varepsilon_{yx} = \varepsilon_{zx} = \varepsilon_{xz} = 0$, where $\omega_p = (4\pi n_p^o e^2/m)^{1/2}$ is the electron plasma frequency. Using Maxwell's equation, the radial component of the electric field can be expressed in terms of the axial component as

$$E_r = -\frac{ik}{\alpha^2}\frac{\partial E_z}{\partial r}, \tag{10}$$

where $\alpha^2 = k^2-\omega^2/c^2$. Taking the z-component of equation (9) and using equations (6) and (10), we obtain

$$\frac{\partial^2E_z}{\partial r^2}+\frac{1}{r}\frac{\partial E_z}{\partial r}-\beta^2E_z = -\frac{\omega_{pb}^2\delta(r-a_1)\alpha^2E_z}{(\omega-kv_{ob})^2}, \tag{11}$$

where $\omega_{pb} = (4\pi N_b e^2/m)^{1/2}$ is the beam plasma frequency and $\beta^2 = \alpha^2\varepsilon_{zz}$.

Similarly, from the third and fourth Maxwell's equations, the wave equation for the z-component of H can be obtained, as the z-component of the curl of the beam current vanishes, as

$$\frac{\partial^2H_z}{\partial r^2}+\frac{1}{r}\frac{\partial H_z}{\partial r}-\alpha^2H_z = 0. \tag{12}$$

In the case of an unmagnetized plasma, equations (11) and (12) are still valid with $\beta = \alpha_1$, $\alpha_1^2 = k^2+\omega_p^2/c^2-\omega^2/c^2$ inside the plasma and $\alpha^2 = k^2-\omega^2/c^2$ outside it. We consider three distinct cases.

Case 1. Strongly magnetized plasma with $\omega_p < \omega$. In this case, when one ignores the beam contribution, equations (11) and (12) have the solutions

$$\begin{aligned} E_z &= A_1'I_o(\beta r), \quad r<a,\\ &= A_2'K_o(\alpha r), \quad r>a, \end{aligned} \tag{13}$$

$$\begin{aligned} H_z &= A_3'I_o(\alpha r), \quad r<a,\\ &= A_4'K_o(\alpha r), \quad r>a. \end{aligned} \tag{14}$$

The transverse components of electromagnetic fields can be obtained from Maxwell's equations:

$$E_r = -\frac{ik}{\alpha^2}\frac{\partial E_z}{\partial r}, \tag{15}$$

$$E_\phi = \frac{i\omega}{\alpha^2c}\frac{\partial H_z}{\partial r}, \tag{16}$$

$$H_r = \frac{ic}{\omega}\frac{\partial E_\phi}{\partial z}, \tag{17}$$

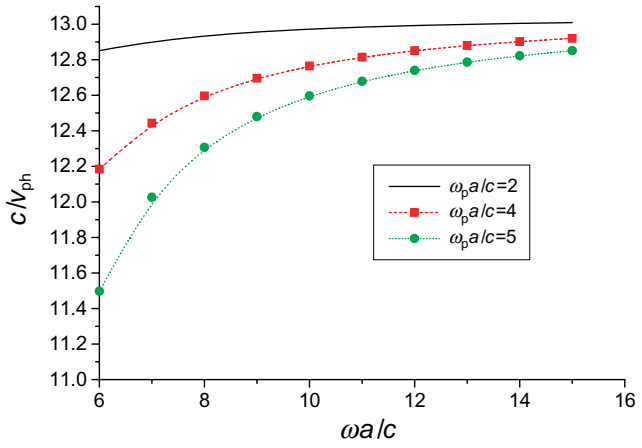

Figure 2. Retardation $c/v_{\rm ph}$ of a shielded helix (a, helix radius) for $\cot\psi = 13$.

$$H_\phi = \frac{\omega}{kc} E_r. \tag{18}$$

The boundary conditions at the anisotropic helix [7, 8] surface ($r = a$) are as follows.

1. E_z and H_z are continuous across the helix surface:

$$\begin{aligned} E_z^i &= E_z^{\rm o}, \\ H_z^i &= H_z^{\rm o}. \end{aligned} \tag{19}$$

2. The electric field disappears in the direction of current flow:

$$E_z^i \sin\psi + E_\phi^i \cos\psi = 0. \tag{20}$$

3. The component of the magnetic field in the direction of conduction is continuous as no current flows perpendicular to it, namely:

$$H_z^i \sin\psi + H_\phi^i \cos\psi = H_z^{\rm o} \sin\psi + H_\phi^{\rm o} \cos\psi. \tag{21}$$

These lead to the dispersion relation for the slow mode

$$\frac{c^2\alpha^3 \tan^2\psi}{\beta\omega^2} = \frac{I_1(\alpha a)K_1(\alpha a)}{I_{\rm o}(\beta a)K_{\rm o}(\alpha a)} \times \left[\frac{K_{\rm o}(\alpha a)I_1(\beta a) + \frac{\alpha}{\beta} I_{\rm o}(\beta a)K_1(\alpha a)}{K_{\rm o}(\alpha a)I_1(\alpha a) + I_{\rm o}(\alpha a)K_1(\alpha a)}\right], \tag{22}$$

with

$$A_2' = \frac{I_{\rm o}(\beta a)}{K_{\rm o}(\alpha a)} A_1', \quad A_3' = \frac{i\alpha c I_{\rm o}(\beta a)\tan\psi}{\omega I_1(\alpha a)} A_1',$$

$$A_4' = \frac{i\alpha c}{\omega} \frac{I_{\rm o}(\beta a) I_{\rm o}(\alpha a)\tan\psi}{K_{\rm o}(\alpha a) I_1(\alpha a)} A_1'.$$

We have solved it numerically for the following parameters: $\cot\psi = 13$, $\omega_{\rm p} a/c = 2$–5. In figure 2, we plot normalized phase velocity $c/v_{\rm ph}$ of the slow mode versus frequency $\omega a/c$ for different $\omega_{\rm p} a/c$ values. For $\omega_{\rm p} a/c = 2$, 4 and 5 the normalized phase velocity $c/v_{\rm ph}$ rises slowly with normalized frequency, attaining saturation at higher $\omega a/c$ values.

Case 2. Strongly magnetized plasma with $\omega_{\rm p} > \omega$. In this case, the solution of equation (11), on neglecting the contribution of the beam, turns out to be

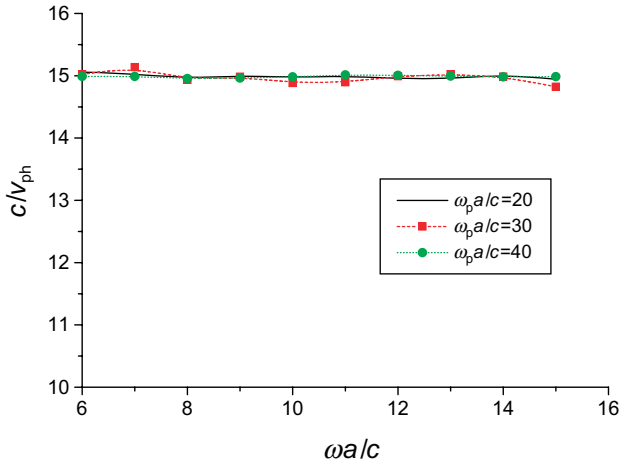

Figure 3. Retardation $c/v_{\rm ph}$ of a shielded helix (a, helix radius) for $\cot\psi = 13$.

$$\begin{aligned} E_z &= A_1' J_{\rm o}(\beta_1 r), \quad r < a, \\ &= A_2' K_{\rm o}(\alpha r), \quad r > a, \end{aligned} \tag{23}$$

where $\beta_1 = (k^2 - \frac{\omega^2}{c^2})(\frac{\omega_{\rm p}^2}{\omega^2} - 1)$. The solution for H_z is still given by equation (14). Applying the boundary conditions as above, one obtains the dispersion relation

$$\frac{c^2\alpha^3 \tan^2\psi}{\beta\omega^2} = -\frac{J_1(\alpha a)K_1(\alpha a)}{J_{\rm o}(\beta_1 a)K_{\rm o}(\alpha a)} \times \left[\frac{K_{\rm o}(\alpha a)J_1(\beta_1 a) - \frac{\alpha}{\beta_1} J_{\rm o}(\beta_1 a)K_1(\alpha a)}{K_{\rm o}(\alpha a)J_1(\alpha a) - J_{\rm o}(\alpha a)K_1(\alpha a)}\right], \tag{24}$$

with

$$A_2' = \frac{J_{\rm o}(\beta a)}{K_{\rm o}(\alpha a)} A_1', \quad A_3' = \frac{i\alpha c J_{\rm o}(\beta a)\tan\psi}{\omega J_1(\alpha a)} A_1',$$

$$A_4' = \frac{i\alpha c}{\omega} \frac{J_{\rm o}(\beta a) J_{\rm o}(\alpha a)\tan\psi}{K_{\rm o}(\alpha a) J_1(\alpha a)} A_1'.$$

We have solved it numerically for $\cot\psi = 13$, $\omega_{\rm p} a/c = 20$–40. Figure 3 shows the variation of normalized phase velocity $c/v_{\rm ph}$ of the slow mode versus frequency $\omega a/c$ for different $\omega_{\rm p} a/c$ values. One may note that the phase velocity of the slow mode does not vary appreciably as the normalized frequency goes from 6 to 16. It also does not vary much as $\omega_{\rm p} a/c$ goes from 20 to 40. However, the phase velocity is larger than in the case of no plasma.

Case 3. Unmagnetized plasma. In the case of unmagnetized plasma, the dielectric constant becomes scalar and $\nabla \cdot \vec{E} = 0$, so the wave equation (11) takes the form

$$\frac{\partial^2 E_z}{\partial r^2} + \frac{1}{r}\frac{\partial E_z}{\partial r} - \alpha'^2 E_z = -\frac{\omega_{\rm pb}^2 \omega^2 \delta(r-a) E_z}{(\omega - k v_{\rm ob})^2 c^2}, \tag{25}$$

where $\alpha'^2 = \alpha_1^2$ for $r < a$, $\alpha_1^2 = k^2 - (\omega^2 - \omega_{\rm p}^2)/c^2$ and $\alpha'^2 = \alpha^2$ for $r > a$. Solving equation (25), one obtains

$$\begin{aligned} E_z &= A_5' I_{\rm o}(\alpha_1 r), \quad r < a, \\ &= A_6' K_{\rm o}(\alpha r), \quad r > a. \end{aligned} \tag{26}$$

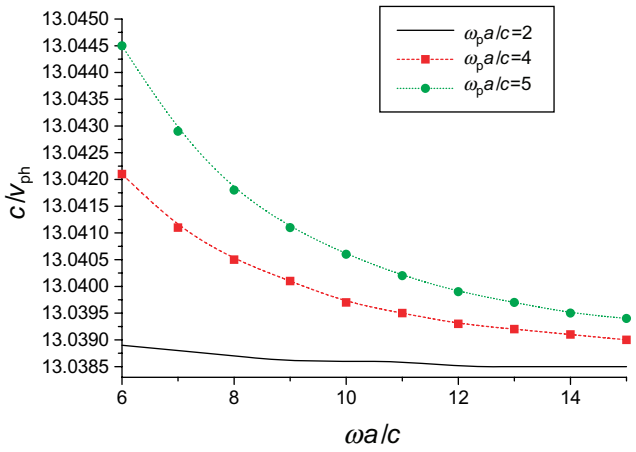

Figure 4. Retardation $c/v_{\rm ph}$ of a shielded helix (a, helix radius) for $\cot\psi = 13$.

Similarly, for H_z

$$\begin{aligned} H_z &= A_7' I_o(\alpha r), \quad r < a, \\ &= A_8' K_o(\alpha r), \quad r > a. \end{aligned} \tag{27}$$

The dispersion relation obtained in this case is

$$\frac{c^2\alpha^3 \tan^2\psi}{\alpha_1\omega^2} = \frac{I_1(\alpha a)K_1(\alpha a)}{I_o(\alpha_1 a)K_o(\alpha a)} \times \left[\frac{K_o(\alpha a)I_1(\alpha_1 a) + \frac{\alpha}{\alpha_1} I_o(\alpha_1 a)K_1(\alpha a)}{K_o(\alpha a)I_1(\alpha a) + I_o(\alpha a)K_1(\alpha a)}\right]. \tag{28}$$

We have solved it numerically for $\cot\psi = 13$ and $\omega_p a/c = 20$–40. Figure 4 shows the variation of normalized phase velocity $c/v_{\rm ph}$ of the slow mode versus frequency $\omega a/c$ for different $\omega_p a/c$ values. For $\omega_p a/c = 2$, 4 and 5 the normalized phase velocity $c/v_{\rm ph}$ decreases with normalized frequency, attaining saturation at higher $\omega a/c$ values. However, the phase velocity is larger than in the case of no plasma.

4. Growth rate

Case 1. Strongly magnetized plasma with $\omega_p < \omega$. With the finite beam term, we presume that the mode structures remain unmodified and only the eigenfrequencies are modified. Thus, we write

$$\begin{aligned} \vec{E} &= A_1(t)\vec{E}_s, \\ \vec{H} &= A_2(t)\vec{H}_s, \end{aligned} \tag{29}$$

where

$$\begin{aligned} E_{sz} &= A_1' I_o(\beta r) e^{-i(\omega t - kz)}, \quad r < a, \\ &= \frac{A_2'}{A_1'} K_o(\alpha r) e^{-i(\omega t - kz)}, \quad r > a, \end{aligned} \tag{30}$$

$$\begin{aligned} H_{sz} &= \frac{A_3'}{A_1'} I_o(\alpha r) e^{-i(\omega t - kz)}, \quad r < a, \\ &= \frac{A_4'}{A_1'} K_o(\alpha r) e^{-i(\omega t - kz)}, \quad r > a, \end{aligned} \tag{31}$$

and where $\vec{E}_s$ and $\vec{H}_s$ represent the mode structures of the electromagnetic fields and satisfy Maxwell's equations without the beam term,

$$\nabla \times \vec{E}_s = -\frac{i\omega}{c}\vec{H}_s,$$

$$\nabla \times \vec{H}_s = -\frac{i\omega}{c}\underline{\underline{\varepsilon}} \cdot \vec{E}_s.$$

Using equation (29) in Maxwell's equation $\nabla \times \vec{E} = -(1/c)(\partial\vec{H}/\partial t)$, one obtains

$$A_1(t)\nabla \times \vec{E}_s = -\frac{1}{c}A_2(t)\frac{\partial \vec{H}_s}{\partial t} - \frac{1}{c}\frac{\partial A_2(t)}{\partial t}\vec{H}_s \tag{32}$$

or

$$\frac{\partial A_2(t)}{\partial t} = -i\omega\,(A_1(t) - A_2(t))\,. \tag{33}$$

Since variation of $\partial/\partial t$ is slow as compared to $i\omega$, equation (33) implies that

$$A_1(t) \approx A_2(t) \quad \text{or} \quad \frac{\partial A_1}{\partial t} \approx \frac{\partial A_2}{\partial t}. \tag{34}$$

Similarly, from the fourth Maxwell's equation

$$\nabla \times \vec{H} = \frac{4\pi \vec{J}_b}{c} + \frac{1}{c}\underline{\underline{\varepsilon}}\cdot\frac{\partial \vec{E}}{\partial t}. \tag{35}$$

Using equations (31) and (34) and taking the z-component, one obtains

$$\frac{\partial A_1(t)}{\partial t}\varepsilon_{zz}E_{sz} = -4\pi J_{bz}, \tag{36}$$

where E_{sz} is the z-component of $\vec{E}_s$. Multiplying both sides by $E_{sz}^* r\,dr$ and integrating over r from $r = 0$ to ∞, we obtain

$$\frac{\partial A_1(t)}{\partial t} = -\frac{4\pi\int_0^\infty J_{bz}E_{sz}^* r\,dr}{\varepsilon_{zz}\int_0^\infty E_{sz}E_{sz}^* r\,dr} = \frac{\omega_{pb}^2\omega a^2\left|E_{sz}^2\right|_{r=a}}{(\omega - kv_{ob})^2 F_1 \varepsilon_{zz}}A_1, \tag{37}$$

where

$$F_1 = \int_0^\infty E_{sz}E_{sz}^* r\,dr = \int_0^a I_o^2(\beta r) r\,dr + \frac{I_o^2(\beta a)}{K_o^2(\alpha a)}\int_0^\infty K_o^2(\alpha r) r\,dr.$$

One may note that the resonant contribution from the beam comes when $\omega = kv_{ob}$. The growth of the wave leads to amplitude being a function of time. Thus we write $\omega = \omega_r + \delta$, $\omega_r = kv_{ob}$, $\partial A_1/\partial t = i\delta A_1$. Then equation (37) gives

$$\delta = \left(\frac{\omega_{pb}^2\omega G}{\varepsilon_{zz}}\right)^{1/3} e^{i(2l+1)\pi/3}, \tag{38}$$

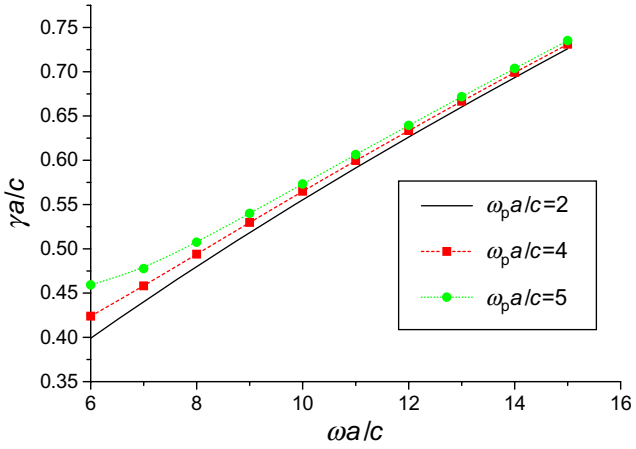

Figure 5. Growth rate for $\omega_p < \omega$ for cot $\psi = 13$.

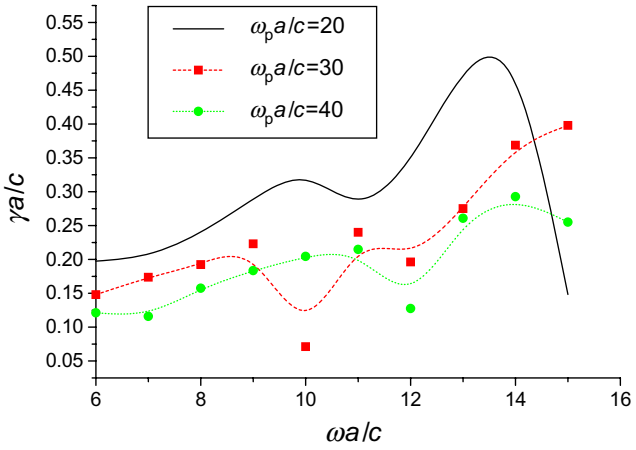

Figure 6. Growth rate for $\omega_p > \omega$ for cot $\psi = 13$.

where $G = \frac{|E_{sz}|^2 a}{F_1}$, in which l is an integer. For $l = 0$, one obtains a growing mode with growth rate $\gamma = \mathrm{Im}(\delta)$ as

$$\gamma = \frac{\sqrt{3}}{2}\left[\frac{\omega_{pb}^2 \omega G}{\varepsilon_{zz}}\right]^{1/3}. \tag{39}$$

We have plotted in figure 5 the variation of growth rate as a function of normalized frequency. The growth rate increases with frequency. As one increases the plasma frequency, the growth rate is enhanced. This is because the mode has higher field concentration inside the helix than outside.

Case 2. Strongly magnetized plasma with $\omega_p > \omega$. For $\omega_p > \omega$, by following the steps given above, one obtains

$$\gamma = \frac{\sqrt{3}}{2}\left[-\frac{\omega_{pb}^2 \omega G'}{\varepsilon_{zz}}\right]^{1/3}, \tag{40}$$

where

$$G' = \frac{|E_{sz}|^2 a^2}{F_2},$$

$$F_2 = \int_0^\infty E_{sz} E_{sz}^* r \, \mathrm{d}r = \int_0^a J_o^2(\beta_1 r) r \, \mathrm{d}r + \frac{J_o^2(\beta_1 a)}{K_o^2(\alpha a)} \int_a^\infty K_o^2(\alpha r) r \, \mathrm{d}r.$$

The variation of growth rate with frequency is shown in figure 6. The growth rate shows oscillatory behaviour and decreases with an increase in plasma density for $\omega_p > \omega$.

Case 3: Unmagnetized plasma. In this case, one obtains

$$\gamma = \frac{\sqrt{3}}{2}\left[\frac{\omega_{pb}^2 \omega G}{\left(1 - \frac{\omega_p^2}{\omega^2}\right)}\right]^{1/3}, \tag{41}$$

where

$$G = \frac{|E_{sz}|^2 a^2}{F_3},$$

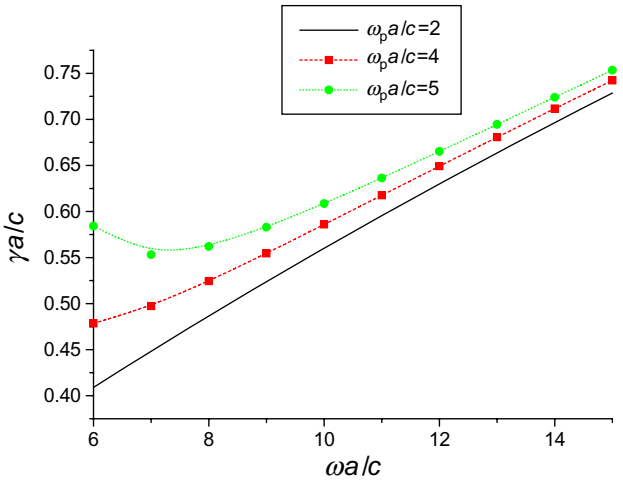

Figure 7. Growth rate for unmagnetized plasma for cot $\psi = 13$.

$$F_3 = \int_0^\infty E_{sz} E_{sz}^* r \, \mathrm{d}r = \int_0^a I_o^2(\alpha_1 r) r \, \mathrm{d}r + \frac{I_o^2(\alpha_1 a)}{K_o^2(\alpha a)} \int_0^\infty K_o^2(\alpha r) r \, \mathrm{d}r.$$

We have plotted in figure 7 the variation of growth rate as a function of normalized frequency. The growth rate increases with frequency. As one increases the plasma frequency, the growth rate is enhanced. This is because the mode has higher field concentration inside the helix than outside it.

5. Results and discussion

The presence of a strongly magnetized plasma drastically changes the mode structure of the azimuthally symmetric mode at $\omega_p = \omega$. For $\omega_p < \omega$ the mode is evanescent in r inside as well as outside the helix. For $\omega_p > \omega$, the axial electric field has a Bessel function behaviour in the interior and modified Bessel function behaviour outside the helix. The axial magnetic field has modified Bessel function behaviour both inside and outside. For $\omega_p < \omega$, as one raises ω_p/ω both the phase velocity and the growth rate increase. For $\omega_p > \omega$, the phase velocity is suppressed, while the growth rate varies in an irregular manner, showing an overall decrease. For an

unmagnetized plasma, the mode is more strongly localized close to the helix and the growth rate increases.

The phase velocity of the unstable mode is slightly lower than the beam velocity. As the beam loses energy to the wave and its average velocity falls down to the phase velocity of the mode, the growth of the microwave should stop. From this, one may have a rough estimate of efficiency as

$$\eta = (\tfrac{1}{2}mv_{ob}^2 - \tfrac{1}{2}m(\omega/k)^2)/(\tfrac{1}{2}mv_{ob}^2) \approx \delta_r/\omega \approx 2\gamma/\sqrt{3\omega}.$$

By tapering the helix, one may have a higher efficiency.

Acknowledgments

One of the authors, Manish Kumar, is grateful to the Banaras Hindu University, India, for financial support.

References

[1] Liu C S and Tripathi V K 2007 *Electromagnetic Theory for Telecommunications* (Cambridge: Cambridge University Press) chapter 3
[2] Choe J Y, Uhm H S and Ahn S 1981 *J. Appl. Phys.* **52** 7067
[3] Uhm H S and Choe J Y 1982 Properties of the electromagnetic wave propagation in a helix loaded waveguide *J. Appl. Phys.* **53** 8483–8
[4] Chu L J and Jackson J D 1948 *Proc. IRE* **36** 853
[5] Tripathi V K 1984 Excitation of electromagnetic waves by an axial electron beam in a slow wave structure *J. Appl. Phys.* **56** 1953–8
[6] Talukdar I and Tripathi V K 1989 Excitation of whistler modes in a sheath helix loaded waveguide *J. Appl. Phys.* **65** 1479–83
[7] Pant K K and Tripathi V K 1992 Excitation of hybrid electrostatic-electromagnetic modes in a plasma-loaded sheath helix *IEEE Trans. Plasma Sci.* **20** 973–8
[8] Chatterjee R 1994 *Elements of Microwave Engineering* (New Delhi: Affiliated East-West Press Pvt Ltd) chapter 9